The role and mechanism of epidermal growth factor receptor in hemodynamic induction of abdominal aortic aneurysm formation

Leiting Liu[1#], Honglin Wang[2#], Xi Chen[1], Yangcheng Zhao[3]

[1]Department of Vascular Surgery, Wuhan No. 1 Hospital, Wuhan, China; [2]Department of Interventional Medicine, Dazhou Central Hospital, Dazhou, China; [3]Department of Peripheral Vascular Intervention, The Affiliated Changsha Central Hospital, Hengyang Medical School, University of South China, Changsha, China

Contributions: (I) Conception and design: L Liu; (II) Administrative support: H Wang; (III) Provision of study materials or patients: X Chen; (IV) Collection and assembly of data: Y Zhao; (V) Data analysis and interpretation: Y Zhao; (VI) Manuscript writing: All authors; (VII) Final approval of manuscript: All authors.

[#]These authors contributed equally to this work.

Correspondence to: Yangcheng Zhao. Department of Peripheral Vascular Intervention, The Affiliated Changsha Central Hospital, Hengyang Medical School, University of South China, 161 Shaoshan South Road, Changsha 410004, China. Email: zyc410004@sina.com.

Background: Abdominal aortic aneurysm (AAA) is a serious threat to human health, and in the event of aneurysm rupture, the rates of disability and mortality are high. At present, the treatment of AAA mainly includes craniotomy and endovascular therapy. With advances in technology, although the safety of the treatment is improving, there is still a risk associated with surgery. Therefore, the exploration of non-invasive treatment options for aneurysms is worthwhile. The etiology of aneurysms must be investigated to identify the target of non-invasive treatment.

Methods: In the experimental group, bilateral common carotid arteries were ligated, while in the control group, bilateral common carotid arteries were exposed. After 5 days, the rabbits were sacrificed, and the hearts were perfused with normal saline. Smooth muscle cells (SMCs) of abdominal aorta were isolated by enzyme digestion. Total RNA was extracted from SMC samples and detected using an Agilent Rabbit 4×44K Gene Expression Microarray. Then, some genes were selected and real-time polymerase chain reaction (RT-PCR) was conducted to verify the credibility of the chip results. Finally, Gene Ontology (GO) analysis and Kyoto Encyclopedia of Genes and Genomes (KEGG) pathway enrichment analysis were performed. The transcriptome contained in the identified differentially expressed gene (DEG) was analyzed.

Results: Microarray revealed 947 DEGs, of which 617 genes were increased and 330 genes were decreased in the experimental group compared with the control group. The microchips of *PTHLH*, *ENPP1*, *IGF1*, and others were selected to verify the altered genes by PCR.

Conclusions: The gene expression of rabbit abdominal aorta SMCs was significantly changed under high blood flow load. Through data analysis, it was found that some specific genes and transcription factors may play an important role in hemodynamically-induced vascular remodeling.

Keywords: Hemodynamics; abdominal aortic aneurysm (AAA); smooth muscle cells (SMCs); gene microarray; vascular remodeling

Submitted Jul 05, 2022. Accepted for publication Sep 13, 2022.
doi: 10.21037/atm-22-3893
View this article at: https://dx.doi.org/10.21037/atm-22-3893

Introduction

Abdominal aortic aneurysm (AAA) is a degenerative disease characterized by the destruction of the abdominal aortic wall structure and progressive dilation into a pulsing mass (1). Although the incidence of AAA has decreased in recent years, the mortality rate after rupture is still very high (2). Smoking, high blood pressure, gender, and family history are important risk factors for AAA (3). The pathogenesis of AAA is complex, and although many mechanisms participate in its occurrence and development, the specific mechanism of the formation and development of AAA has remained elusive (4). Up to now, various basic studies related to the pathogenesis of AAA and the formulation of an early drug treatment plan are still hot spots of research. An in-depth exploration of the mechanism of AAA is needed to facilitate the development of effective treatment methods. As a common degenerative cardiovascular disease, AAA is a potentially fatal condition. With the improvement of screening technology and the rapid development of endovascular interventional therapy, the mortality rate of AAA has decreased, yet not to a negligible level (5-7). The lack of effective drug treatments for AAA means that its intervention is still surgically dominated. Although the epidemiology, genetics, risk factors, and pathophysiological mechanism of AAA have been studied, there is still no effective drug to prevent and treat AAA (8). Therefore, it is very important to understand the mechanism of AAA occurrence and how to inhibit the pathogenesis of AAA. The pathological changes of an AAA tumor wall include chronic transmural inflammation, destructive reconstruction of extracellular matrix (ECM), and apoptosis of vascular smooth muscle cells (VSMCs), among which the destruction of aneurysm wall ECM is one of the key mechanisms, which is closely related to the matrix metalloproteinase (MMP) family (9-11).

The innate immune system, especially toll-like receptor (TLR), chemokine receptor, and complement, participate in the progression of AAA. The current study involved an in-depth study of the pathophysiological process of AAA and aimed to ascertain effective methods or drugs to block or delay the progression of AAA. Since 2000, the prevalence and incidence of AAA have declined in developed countries, but have increased in some regions and countries, such as Latin America and high-income Asia-Pacific countries (12). The global prevalence of AAA is still unclear, with only a few countries providing reports on the prevalence of AAA. The rate of AAA treatment varies greatly in different regions, which may be related to selection bias, as the affordability and availability of medical resources varies greatly across different populations (13).

The global prevalence of AAA remains unclear, with only a few countries providing reports of AAA prevalence. Treatment rates for AAA vary widely across regions, which may be due to selection bias as the availability and/or access to medical resources vary widely among different populations. AAA is the 12th to 15th leading cause of death among people 55 and older in the United States. Overall mortality was higher in both treated and untreated AAA patients than in the general population, primarily because most AAA patients died from cardiovascular disease rather than from ruptured AAA. In addition to cardiovascular causes of death, cancer is another common cause of death in people with AAA, and given the decline in autopsy rates, it is difficult to determine the true mortality associated with AAA rupture outside the health care setting. Known risk factors for AAA include smoking, high blood pressure, hyperlipidemia, age, gender, and family history. Hypertension often coexists with AAA. Studies (14,15) have found that hypertension can promote the development of AAA; the use of drugs to control blood pressure can significantly slow down the growth and expansion of a pulse tumor. The relationship between lipid levels and AAA is still controversial. Dysfunctions of circulating high-density lipoprotein (HDL) particles have been reported in patients with AAA, and decreased circulating apolipoprotein A1 (major protein component of HDL) and HDL egg white can promote the growth of AAA. A retrospective analysis in the Netherlands suggested that statins could slow the progression of AAA, but this view has not been confirmed in prospective studies.

In conclusion, SMCs are an important link in the pathological process of aneurysm formation, revealing the changes of phenotype. Therefore, they play an important role in deepening the understanding of the pathogenesis of AAA. To investigate SMC expression changes in hemodynamic load, we established a hemodynamic changes-induced rabbit AAA model, applied of gene chip detection technology (16), screened for gene expression changes in hemodynamic load, and explored the genetic variations of bioinformatics analysis, hoping that our findings would provide a clue for further study. We present the following article in accordance with the ARRIVE reporting checklist (available at https://atm.amegroups.com/article/view/10.21037/atm-22-3893/rc).

Methods

Establishment of the animal model

Sixteen New Zealand white rabbits (weight 2.0–3.0 kg, 1–4 months, male, from University of South China Animal Research Center) were randomly assigned into an experimental group and a control group. An injection of 1% pentobarbital at a dose of 20 mg/kg was administered to New Zealand white rabbits through the ear margin vein for anesthetization. Following successful anesthesia, the experimental animals were placed in the supine position on the operating table, and their limbs and heads were fixed with rubber bands. The neck was shaved from the supraclavicular fossa to the mandibular level. Conventional application of iodophor was used alongside alcohol disinfection. An incision of about 2 cm in length was made in the middle of the neck to cut the skin and subcutaneous tissue, and the separation was continued deep along the muscle space until the trachea was exposed. Blunt muscle separation was performed on both sides of the trachea to expose the bilateral carotid sheaths, and the common carotid artery was carefully dissociated to avoid injury to the surrounding veins and vagus nerve. The experimental group underwent ligation of bilateral common carotid arteries, and the control group was sutured after exposure. The anterior neck muscles and skin were sutured intermittently in turn, and the animals were then placed in separate rabbit cages. All the animals were enrolled in the analysis (eight animals in each group). A protocol was prepared before the study without registration. Experiments were performed under a project license (No. 2021-107) granted by the Animal Ethics Committee of the Affiliated Changsha Central Hospital, in compliance with *Guide for the Care and Use of Laboratory Animals*, *8th edition* for the care and use of animals.

Determination of blood flow velocity in rabbit abdominal aortae

The blood flow velocity of the abdominal aorta was measured before and 5 days after operation. The dose rate of 0.1 mL/kg was applied. The muscle of the rabbits was sedated by Su Mian Xin II (ZooMAb). After waiting for about 10 minutes, the abdominal aortic flow rate of rabbits was measured by Philips Medical ultrasound (Philips Healthcare, Andover, MA, USA), and time-averaged peak velocity (TAPV) was recorded.

Measurement of abdominal aorta diameter in rabbits

The control group and the experimental group of rabbits underwent cerebral angiography (Philips Healthcare) 5 days after surgery. According to the dosage of 20 mg/kg, 1% pentobarbital was administered through an auricular vein. After anesthesia, the rabbits were fixed to a homemade board. The skin was prepared at the right femoral artery and disinfected with iodophor and 75% alcohol. After identification of the femoral artery, the skin was cut layer by layer along the femoral artery edge, and the incision length was about 3 cm. The femoral artery was separated and exposed, an arterial puncture needle was used to puncture the femoral artery, and a guide wire was inserted. The guide wire was fixed, the puncture needle was retracted, and a 4-F artery sheath was inserted along the guide wire.

Isolation of SMCs from rabbit abdominal aorta

The rabbits were administered 1% pentobarbital by ear vein injection at 100 mg/kg. In the case of anesthetic overdose, a physiological saline perfusion was immediately applied to the heart for 10 minutes. The aorta vessels were removed and carefully separated under a microscope. The SMCs of rabbit abdominal aortae were isolated according to the reported protocol (17). First, the blood vessels were cleaned with phosphate-buffered saline (PBS), and the residual blood and adhesive tissues were removed. Then, the inner wall of the blood vessels was turned out under the microscope, immersed in PBS containing elastic enzyme (0.4 mg/mL) and type I collagenous A (1 mg/mL), digested at 37 ℃ for 10 minutes, and the inner wall was cleaned with PBS. The endothelial cells are removed and the remaining tissue was then digested with digestive juices for 30 minutes and centrifuged to collect the SMCs.

Extraction and purification of RNA

Total RNA was extracted from the separated SMC samples by TRIzol Reagent (Cat#15596-018, Life Technologies, Carlsbad, CA, USA) according to the manufacturer's standard procedure. Total RNA was extracted and tested by Agilent Bioanalyzer 2100 (Agilent Technologies, Santa Clara, CA, USA). The total RNA was purified using an RNeasy micro kit (Cat#74004, QIAGEN, Hilden, Germany) and an RNase-Free DNase Set (Cat#79254, QIAGEN).

Chip data analysis

There are only a few known genes in rabbits and many sequences have not been reported in the rabbit gene bank.

Before gene application, we consulted Better Bunny (http://cptweb.cpt.wayne.edu/BB/index.php) and conducted gene homology comparison, to investigate whether the homology is greater than or equal to 50% of the genes. Then, with P<0.05 and fold change (FC) >2 as the boundary value, the differential genes between the experimental group and the control group were screened. After deleting the duplicate genes, DAVID software (http://david.abcc.ncifcrf.gov/) was applied, followed by Gene Ontology (GO) for different genes and Kyoto Encyclopedia of Genes and Genomes (KEGG) pathway analysis. Transcriptome and key genes in differential genes were screened and analyzed. The original data of chip results has been uploaded to the National Center for Biotechnology Information (NCBI)'s Gene Expression Omnibus (GEO) with serial number GSE61212.

RNA extraction, reverse transcription, and real-time quantitative polymerase chain reaction (qRT-PCR)

In order to verify the reliability of the gene chip results, qRT-PCR was applied. Four significantly upregulated genes (*PTHLH*, *ENPP1*, *IGF1*, and *GPX7*) and four significantly down-regulated genes (*PRKG1*, *RR-2*, *CACNB2*, and *PTH1R*) were detected by qRT-PCR.

Immunohistochemical staining

Paraffin sections (5-μm thick) extracted from the tissue were dewaxed in xylene, rehydrated in graded alcohol, and endogenous peroxidase activity was blocked by infiltration into 0.3% hydrogen peroxide. Then, to enhance antigen accessibility, sections were heated with 0.1 M citrate buffer (pH6.0) at 121 ℃ for 3 min in an autoclave. After cooling, the endogenous peroxide activity was blocked with hydrogen peroxide (0.3%) for 20 min. Next, sections were rinsed with phosphate buffered saline (PBS) (PH 7.2) and then incubated with DTX3L (CAT) (SC-100627; Santa Cruz Biotechnology Inc., Santa Cruz, CA, USA) and Ki-67 (SC-23900; Santa Cruz Biotechnology) applied antibodies for 2 hours at room temperature. All sections were treated with immunoglobulin IgG as secondary antibody. After washing with PBS, the sections were incubated with DAB (0.02% diaminobenzidine hydrochloric acid, 0.1% phosphate buffer) to observe the peroxidase reaction of H_2O_2. The final sections were stained with hematoxylin, dehydrated with graded alcohol, and mounted on resin supports. The stained sections were examined with a microscope.

Protein-protein interaction (PPI) networks

Using the STRING data library (https://cn.string-db.org) and normal fetal adrenal neuroblastoma organizations the nerve cell tissue multiples |logFC| of 4 or more of the miRNA target genes to build protein interaction network. The protein interaction Network data obtained from STRING were imported into Cytoscape software, and the Network Analyzer plug-in was used to screen out the key target genes with more nodes and construct the PPI core network.

Statistical analysis

The software SPSS 23.0 (IBM Corp., Armonk, NY, USA) was used for statistical and data analysis. Measurement data were expressed as mean ± standard deviation. The comparison of basilar artery diameter between the control group and the experimental group, and the quantitative analysis of IGF1 and TNF-α integrated optical density (IOD) were performed by *t*-test. The RT-PCR data of *IGF1* and *GPX7* were tested for homogeneity of variance, and Kruskal-Wallis H test was used if the two populations were inferred to be unequal. The RT-PCR data of *ENPP1*, *PTHLH*, *PRKG1*, and other genes were consistent with homogeneity of variance test, and *t*-test was used. A P value <0.05 was considered statistically significant.

Results

Changes of blood flow velocity in abdominal aorta before and after modeling

Before modeling and 5 days after modeling, the TAPV of abdominal aortae was measured by ultrasound and analyzed statistically. *Table 1* shows the velocity of the basilar artery in rabbits before and after modeling. The velocity of basilar aneurysm before modeling was 24.59±1.58 cm/s, and that 5 days after modeling was 48.54±10.6 cm/s, which represented an increase of 23.5±3.2 cm/s after modeling (*Table 1*). The difference before and after modeling was statistically significant (P<0.001) (*Figure 1*).

Abdominal aorta diameter changes before and after modeling

After ligation of bilateral common carotid arteries, blood flow in the abdominal aorta increased, leading to significant remodeling of the abdominal aorta.

The diameter of the basal abdominal aorta was measured and calculated 5 days after operation by using a 3.5-mm diameter steel ball placed during angiography as a reference (*Table 2*). The basilar artery diameter was 0.64±0.08 mm in the control group and 0.85±0.07 mm in the experimental group, respectively. After ligation of bilateral common carotid arteries, the diameter of the abdominal aorta increased, and there was a statistical difference between the two groups (P=0.0035, P<0.05) (*Figure 2*). The animals were then euthanized, the blood vessels were removed together with the abdominal aorta, and the abdominal aorta was carefully separated. It was found that the diameter of the experimental group was enlarged and the shape was tortuous compared with that of the control group, which was consistent with the results of angiography.

Table 1 Blood flow velocity of rabbit basilar artery before and after modeling (cm/s)

No.	Before the modeling	5 days after modeling
1	24.2	48.6
2	22.7	38.9
3	25.4	62.1
4	26.3	42.5
5	23.8	59.4
6	24.4	38.7
7	27.1	60.5
8	22.8	37.6

Transcriptional mutations in SMCs of rabbit abdominal aorta

In order to reveal the molecular mechanism of VSMCs in hemodynamically-induced vascular remodeling methods, and we isolated the SMCs from the experimental group and the control group of the abdominal aorta, and carried out gene microarray detection.

In order to better compare the differentially expressed genes (DEGs) between the experimental group and the control group, we used a volcano map to show the DEGs. The three straight lines limited the multiple of change and P value. In the volcano diagram, the red dots represent the DEGs that were more than two times up-regulated in the experimental group and with a P value less than 0.05, and the green dots represent the DEGs that are more than two times down-regulated in the experimental group and with a P value less than 0.05 (*Figure 3*).

DEGs were detected by microarray probe technique

By analyzing the chip results, we found that the SMCs in the experimental group were flowing through the blood

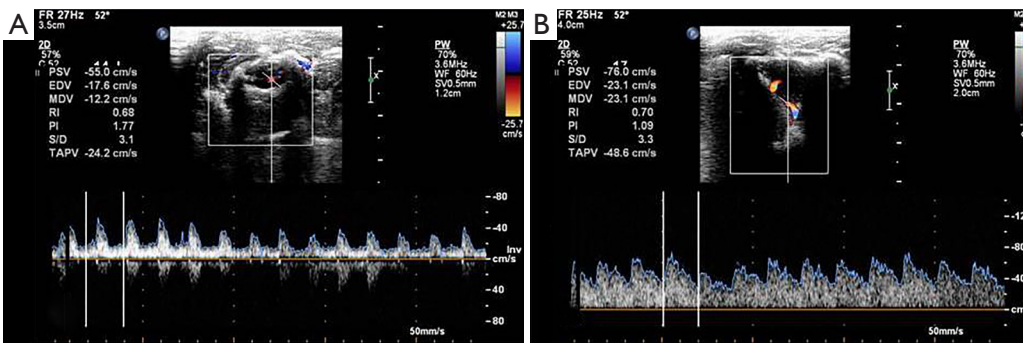

Figure 1 Basilar artery flow velocity before and after modeling [(A) flow velocity before modeling; (B) flow rate 5 days after modeling].

Table 2 Diameter of rabbit abdominal aorta

Project	Diameter of abdominal aorta (mm)				
	Day 1	Day 2	Day 3	Day 4	Day 5
Control group	0.69	0.74	0.64	0.59	0.53
Experimental group	0.85	0.91	0.85	0.74	0.78

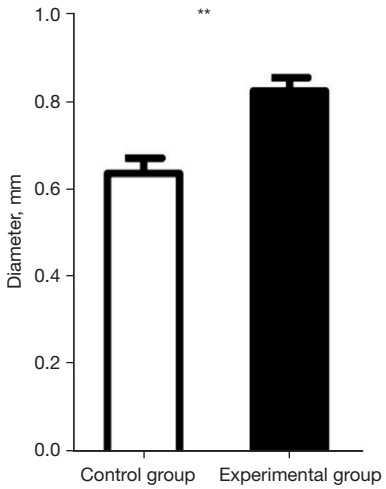

Figure 2 Comparison of basilar artery diameter between the control group and the experimental group. **, P<0.01.

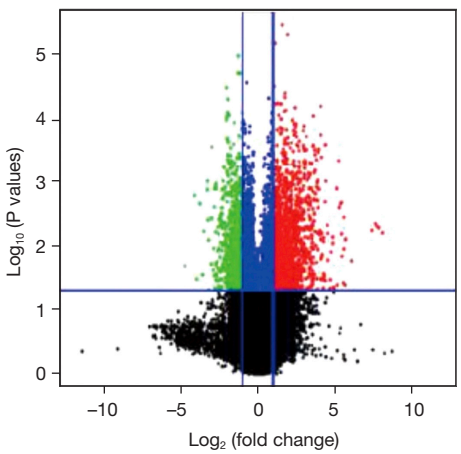

Figure 3 Comparative analysis of differential gene expression. Red: up-regulated gene; green: down-regulated gene; blue: non-regulatory genes; black: negative gene expression.

stream compared to the control group. The results can be used to cluster the differentially expressed genes between the experimental group and the control group. These results indicated that the expression of a large number of genes was significantly altered in vascular smooth muscle cells under the effect of hemodynamics (*Table 3*).

Identification of DEGs

The qRT-PCR detection results of four up-regulated genes (*PTHLH*, *ENPP1*, *IGF1*, and *GPX7*) and four down-regulated genes (*PRKG1*, *RR-2*, *CACNB2*, and *PTH1R*) showed that genes that were up-regulated in the microarray results were also up-regulated in RT-PCR results, and genes that were down-regulated in the microarray results were also down-regulated in RT-PCR results. Multiple changes of genes were detected by RT-PCR in chip results. Although the multiples of their changes are slightly different, the trend of changes was the same, which supports the reliability of the chip results (*Table 4*).

Analysis of immunohistochemical results

We randomly selected five high-magnification microscope fields and counted at least 300 cells per section. The percentage of positive tumor cells was 10–49%, 25–74%, 37.5–100%. Staining intensity was estimated and scored as follows: 0, no staining; 1, weak staining; 2, medium staining; 3, strong staining. Combining the scores of the two scales, we divided each part into the following categories: 0–4.5 denotes low expression; 4.5–9 indicates high expression (*Figure 4*).

PPI analysis

Target genes were imported into STRING database to

Table 3 Number of differential genes detected by chip probe

Genes	Mutant gene	Up-regulation	Down-regulation	Change a multiple	P value
PRKG1	43,603	20,374	23,227	–	0.01
RR-2	1,648	897	751	–	0.01
CACNB2	988	672	316	2	0.01
PTH1R	5,070	2,437	2,633	–	0.05
GPX7	2,250	1,470	780	2	0.05

construct protein interaction network map. The Cytoscape software Network Analyzer plug-in was used to sort the key target genes with the most nodes according to the number of gene nodes, and the PPI core Network map was constructed (*Figure 5*).

Discussion

The continuous increase of AAA due to deterioration of the arterial wall is called "growth" of AAA (18). The average growth rate of AAA is 2.5 mm per year, which is 20–25% faster in smokers and 25% slower in diabetics, which may be related to metformin treatment or ECM conversion changes. The majority of aneurysm increase over time, but a small percentage of patients have undetectable increases in AAA, which may also be influenced by testing methods. Factors associated with AAA growth include high blood pressure, gender, and chronic obstructive pulmonary disease (19). Patients with AAA who are clinically undiagnosed or diagnosed but not monitored are at increased risk of rupture and potentially fatal hemorrhages (20). Therefore, confirmed AAA patients should be monitored. Factors affecting AAA rupture include aneurysm size and morphology: an AAA diameter >55 mm is more likely to rupture, and AAA diameter is often used to predict the risk of AAA rupture in clinical practice (21-24). However, the accuracy of predicting the risk of AAA rupture based on AAA diameter is controversial, as monitoring of vessel diameter shows that even an AAA diameter <55 mm is likely to rupture. Studies have confirmed that women with AAA have a higher risk of rupture than men, and smokers and those with untreated hypertension are also at increased risk (25-27). It is still a hot research topic to assess the specific rupture risk of patients with AAA by monitoring aneurysm volume, aortic size index (ratio of body surface area to aneurysm diameter), family history of AAA, diabetes mellitus, and biomarkers. Specific inhibitors

Table 4 Expression changes of *IGF1* and *TNF-α* in chip detection

Gene	Multiple of difference (experimental group *vs.* control group)	P value
IGF1	5.49	0.00018
TNF-α	3.65	0.03584

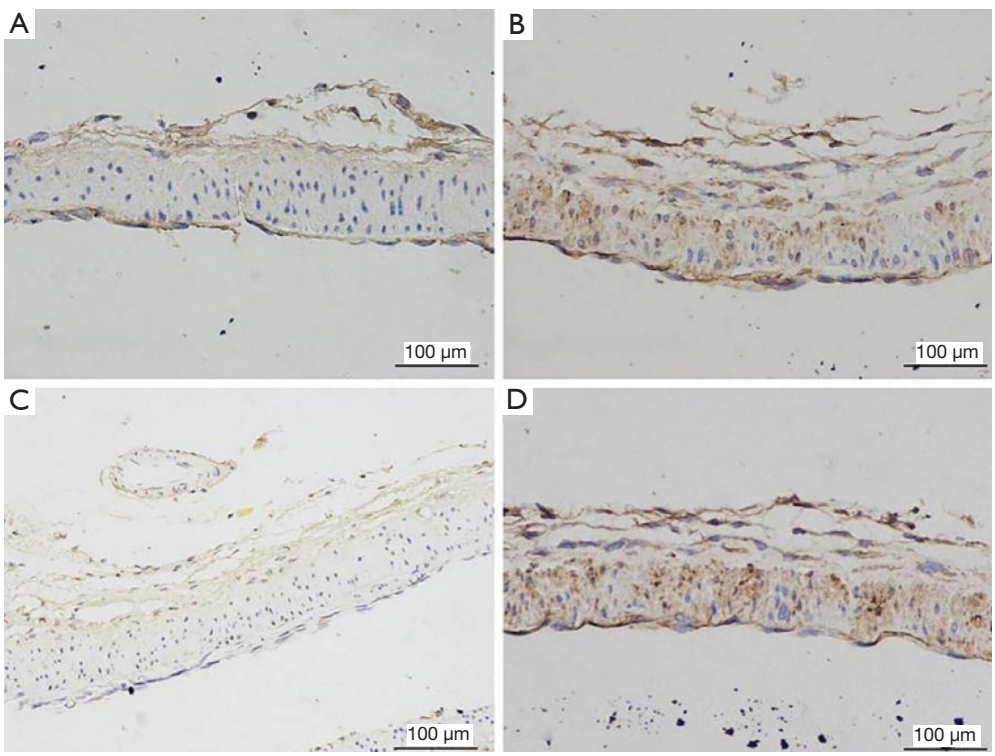

Figure 4 Abdominal aorta was stained with *IGF1* and *TNF-α* immunohistochemistry.

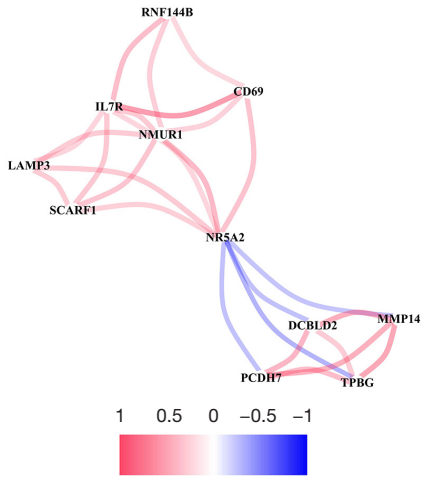

Figure 5 PPI network correlation analysis results. PPI, protein-protein interaction.

of de integrin and metalloproteinase 10 can significantly reduce the incidence of AAA and abdominal aortic diameter in angiotensin II-induced apolipoprotein E deficient mice, which makes it possible to treat AAA by regulating de integrin and metalloproteinase 10. The long-term effects need to be further studied. The increased risk of aortic rupture in women compared to expected aortic diameter may be associated with a relatively large aortic size index (28).

Disruption of the ECM is one of the key pathophysiological mechanisms of AAA, and MMPs is most closely related to this mechanism. MMPs is a series of enzymes that can degrade various ECM components, which can degrade collagen and elastic egg white components in abdominal aortic wall tissue, leading to arterial wall remodeling, and then gradually expand the arterial wall to form aneurysms. Overexpression of MMPs exists in AAA, including MMP-2 and MMP-9. Overexpression of MMPs can degrade type IV gliadin, proteoglycan core protein, and elastin, leading to the occurrence of aneurysms. With the increase of the level of MMP-9 proenzyme in AAA, the activity of proteolytic enzyme increased, and with the increase of the level of MMP-9 proenzyme, the risk of AAA rupture increased. After AAA was repaired, the level of MMP-9 decreased significantly. If MMP-9 levels remain high in AAA patients after endovascular or open treatment, the risk of continued development or leakage of repaired aneurysms is increased. Further, MMP-2 can also shear elastin and type IV collagen. Studies (29,30) have shown that MMP-2 and MMP-9 are interdependent and synergistic in the progression of AAA. In addition to MMP-2 and MMP-9, whether other MMPs are involved in the pathogenesis of aneurysms should be further studied. Epidermal growth factor (EGF) is one of the earliest growth factors, which plays an important role in regulating cell growth, proliferation and differentiation. EGF is a small peptide. In humans, EGF protein has 53 amino acid residues and three disulfide bonds. Alanine, phenylalanine, and lysine are not present in the peptides. It has three disulfide bonds, these disulfide bonds are necessary for its biological activity, such as adding leucyl reagent and urea, EGF is inactivated, the sulfhydryl group on the peptide chain can be naturally oxidized in air and fully restored activity. EGFR (epithelial growth factor receptor) itself has tyrosine kinase activity. Once combined with EGF, EGFR can activate related genes in the nucleus to promote cell division and proliferation. EGFR expression was increased in gastric cancer, breast cancer, bladder cancer and head and neck squamous cell carcinoma.

Apoptosis of VSMC is the main cell formation of aortic wall middle membrane, and can promote the synthesis of elastin, collagen, and other ECM, which is the basis of guaranteeing the normal vasomotor function (31). Depletion of VSMC is an obvious pathological sign of advanced aneurysms. Reduced number of VSMC is one of the reasons for the formation of AAA, and reduced number of VSMC is due to apoptosis. Loss of VSMC is also a sentinel feature of experimental aneurysm (32). Part of the disappearance of VSMC is caused by the enhanced hydrolysis of egg white on aortic wall and the change of oxidative environment. Seraminase, plasminase, and elastase can induce apoptosis of VSMC, and intense oxidative stress can also induce apoptosis of VSMC. Ceroids (yellowish-brown polymers composed of oxidized lipids and proteins) are highly toxic to VSMC and can lead to increased oxidative stress and apoptosis of VSMC (33). They are present in the wall of AAA tumors.

Metabolic disorders increase the risk of AAA. NRs (nuclear hormone receptors) are increasingly recognized as important regulators of cellular metabolism. However, the role of NRs in AAA development remains largely unknown. AAA is a life-threatening condition characterized by permanent local dilation of the abdominal aorta, leading to a catastrophic event of rupture and sudden death. Most patients with AAA are asymptomatic until a fatal rupture, which hinders early diagnosis of AAA. Currently, open surgical repair and endovascular placement of stent grafts are the mainstay of treatment for AAA, and there are no Food and Drug Administration-approved drug therapies

to limit progression or reduce rupture risk. To identify new therapeutic targets, it is essential to gain insight into the underlying molecular mechanisms that regulate AAA formation and progression. Metabolic pathways, including glucose, lipid, and amino acid metabolism, have integral roles in normal and dysfunctional vasculature. As the power source of the cell, mitochondria play an important role in regulating these metabolic pathways through tricarboxylic acid (TCA) cycling and oxidative phosphorylation, and strict control of mitochondrial function is essential to maintain metabolic homeostasis. A recent single-cell RNA sequencing study (34) showed that extensive mitochondrial dysfunction occurs in different aortic cell types and is a feature of aortic aneurysms. However, the regulatory mechanisms of mitochondrial metabolic pathways in aortic aneurysm development remain poorly understood.

Hemodynamics plays an important role in the formation of AAA. Exploration of hemodynamic changes in depth and the effect on blood vessels can help us further understand the mechanism of AAA. The SMCs are the main component of intracranial vascular wall, and the inflammatory factors secreted by SMCs such as MMPs can induce the inflammatory response of vascular wall and the destruction of vascular wall matrix, and eventually lead to the protrusions of vascular wall and aneurysm (35). Limitation: This was an animal study, and the results needed to be confirmed in human study. Changes in the expression profile of SMCs under high hemodynamic load *in vivo* have not been reported. In this study, an animal model of ligation of bilateral common carotid arteries in rabbits to improve the blood flow load of abdominal aorta was used to isolate SMCs in abdominal aorta, extract RNA for gene chip detection, and conduct bioinformatics analysis of DEGs.

Acknowledgments

Funding: None.

Footnote

Reporting Checklist: The authors have completed the ARRIVE reporting checklist. Available at https://atm.amegroups.com/article/view/10.21037/atm-22-3893/rc

Data Sharing Statement: Available at https://atm.amegroups.com/article/view/10.21037/atm-22-3893/dss

Conflicts of Interest: All authors have completed the ICMJE uniform disclosure form (available at https://atm.amegroups.com/article/view/10.21037/atm-22-3893/coif). The authors have no conflicts of interest to declare.

Ethical Statement: The authors are accountable for all aspects of the work in ensuring that questions related to the accuracy or integrity of any part of the work are appropriately investigated and resolved. Experiments were performed under a project license (No. 2021-107) granted by the Animal Ethics Committee of the Affiliated Changsha Central Hospital, in compliance with *Guide for the Care and Use of Laboratory Animals*, *8th edition* for the care and use of animals.

References

1. Sabbah DA, Hajjo R, Sweidan K. Review on Epidermal Growth Factor Receptor (EGFR) Structure, Signaling Pathways, Interactions, and Recent Updates of EGFR Inhibitors. Curr Top Med Chem 2020;20:815-34.
2. Harrison PT, Vyse S, Huang PH. Rare epidermal growth factor receptor (EGFR) mutations in non-small cell lung cancer. Semin Cancer Biol 2020;61:167-79.
3. Peterson JL, Ceresa BP. Epidermal Growth Factor Receptor Expression in the Corneal Epithelium. Cells 2021;10:2409.
4. Trivedi S, Ferris RL. Epidermal Growth Factor Receptor-Targeted Therapy for Head and Neck Cancer. Otolaryngol Clin North Am 2021;54:743-9.
5. Martinelli E, Ciardiello D, Martini G, et al. Implementing anti-epidermal growth factor receptor (EGFR) therapy in metastatic colorectal cancer: challenges and future perspectives. Ann Oncol 2020;31:30-40.
6. Masood A, Kancha RK, Subramanian J. Epidermal growth factor receptor (EGFR) tyrosine kinase inhibitors in non-small cell lung cancer harboring uncommon EGFR mutations: Focus on afatinib. Semin Oncol 2019;46:271-83.

7. Ayati A, Moghimi S, Salarinejad S, et al. A review on progression of epidermal growth factor receptor (EGFR) inhibitors as an efficient approach in cancer targeted therapy. Bioorg Chem 2020;99:103811.
8. Wu L, Zheng Y, Liu J, et al. Comprehensive evaluation of the efficacy and safety of LPV/r drugs in the treatment of SARS and MERS to provide potential treatment options for COVID-19. Aging (Albany NY) 2021;13:10833-52.
9. Chia PL, Scott AM, John T. Epidermal growth factor receptor (EGFR)-targeted therapies in mesothelioma. Expert Opin Drug Deliv 2019;16:441-51.
10. Mushtaq U, Bashir M, Nabi S, et al. Epidermal growth factor receptor and integrins meet redox signaling through P66shc and Rac1. Cytokine 2021;146:155625.
11. Sharma B, Singh VJ, Chawla PA. Epidermal growth factor receptor inhibitors as potential anticancer agents: An update of recent progress. Bioorg Chem 2021;116:105393.
12. Grapa CM, Mocan T, Gonciar D, et al. Epidermal Growth Factor Receptor and Its Role in Pancreatic Cancer Treatment Mediated by Nanoparticles. Int J Nanomedicine 2019;14:9693-706.
13. Bao SM, Hu QH, Yang WT, et al. Targeting Epidermal Growth Factor Receptor in Non-Small-Cell-Lung Cancer: Current State and Future Perspective. Anticancer Agents Med Chem 2019;19:984-91.
14. Zanwar S. Epidermal growth factor receptor mutated lung cancers: Looking beyond adenocarcinomas. Indian J Cancer 2021;58:3-4.
15. London M, Gallo E. Epidermal growth factor receptor (EGFR) involvement in epithelial-derived cancers and its current antibody-based immunotherapies. Cell Biol Int 2020;44:1267-82.
16. Golledge J. Abdominal aortic aneurysm: update on pathogenesis and medical treatments. Nat Rev Cardiol 2019;16:225-42.
17. Wang YD, Liu ZJ, Ren J, et al. Pharmacological Therapy of Abdominal Aortic Aneurysm: An Update. Curr Vasc Pharmacol 2018;16:114-24.
18. Powell JT, Wanhainen A. Analysis of the Differences Between the ESVS 2019 and NICE 2020 Guidelines for Abdominal Aortic Aneurysm. Eur J Vasc Endovasc Surg 2020;60:7-15.
19. Yuan Z, Lu Y, Wei J, et al. Abdominal Aortic Aneurysm: Roles of Inflammatory Cells. Front Immunol 2021;11:609161.
20. Fabiani MA, González-Urquijo M, Riambau V, et al. EVAR Approach for Abdominal Aortic Aneurysm with Horseshoe Kidney: A Multicenter Experience. Ann Vasc Surg 2019;58:232-7.
21. Peeters B, Moreels N, Vermassen F, et al. Management of abdominal aortic aneurysm and concomitant malignant disease. J Cardiovasc Surg (Torino) 2019;60:468-75.
22. Braet DJ, Eliason J, Ahmed Y, et al. Vascular Deformation Mapping of Abdominal Aortic Aneurysm. Tomography 2021;7:189-201.
23. Torres-Fonseca M, Galan M, Martinez-Lopez D, et al. Pathophisiology of abdominal aortic aneurysm: biomarkers and novel therapeutic targets. Clin Investig Arterioscler 2019;31:166-77.
24. Wu L, Zheng Y, Ruan X, et al. Long-chain noncoding ribonucleic acids affect the survival and prognosis of patients with esophageal adenocarcinoma through the autophagy pathway: construction of a prognostic model. Anticancer Drugs 2022;33:e590-e603.
25. Gandhi R, Bell M, Bailey M, et al. Prospect of positron emission tomography for abdominal aortic aneurysm risk stratification. J Nucl Cardiol 2021;28:2272-82.
26. Stoberock K, Kölbel T, Atlihan G, et al. Gender differences in abdominal aortic aneurysm therapy - a systematic review. Vasa 2018;47:267-71.
27. Spanos K, Nana P, Behrendt CA, et al. Management of Abdominal Aortic Aneurysm Disease: Similarities and Differences Among Cardiovascular Guidelines and NICE Guidance. J Endovasc Ther 2020;27:889-901.
28. Gonzalez-Urquijo M, de Zamacona RG, Mendoza AKM, et al. 3D Modeling of Blood Flow in Simulated Abdominal Aortic Aneurysm. Vasc Endovascular Surg 2021;55:677-83.
29. Coles-Black J, Bolton D, Robinson D, et al. Utility of 3D printed abdominal aortic aneurysm phantoms: a systematic review. ANZ J Surg 2021;91:1673-81.
30. Tanaka H. Problems and Perspectives of Abdominal Aortic Aneurysm Research. Curr Drug Targets 2018;19:1227.
31. Raffort J, Adam C, Carrier M, et al. Artificial intelligence in abdominal aortic aneurysm. J Vasc Surg 2020;72:321-333.e1.
32. Ambler GK, Twine CP. Abdominal Aortic Aneurysm Repair in Advanced Age: Is Age Really the Problem? Eur J Vasc Endovasc Surg 2021;61:929.
33. Summerhill VI, Sukhorukov VN, Eid AH, et al. Pathophysiological Aspects of the Development of Abdominal Aortic Aneurysm with a Special Focus on Mitochondrial Dysfunction and Genetic Associations. Biomol Concepts 2021;12:55-67.
34. Yue J, Yin L, Shen J, et al. A Modified Murine

Abdominal Aortic Aneurysm Rupture Model Using Elastase Perfusion and Angiotensin II Infusion. Ann Vasc Surg 2020;67:474-81.
35. Ivanov LN, Maksimov AL, Mukhin SA, et al. Surgical treatment of patients with abdominal aortic aneurysm and ischaemic heart disease. Angiol Sosud Khir 2021;27:85-93.

(English Language Editor: J. Jones)

Cite this article as: Liu L, Wang H, Chen X, Zhao Y. The role and mechanism of epidermal growth factor receptor in hemodynamic induction of abdominal aortic aneurysm formation. Ann Transl Med 2022;10(18):1002. doi: 10.21037/atm-22-3893

